

Beading instability and spreading kinetics in grooves with convex curved sides

Patrick B. Warren*

Unilever R&D Port Sunlight, Quarry Road East, Bebington, Wirral, CH63 3JW, UK.

(Dated: December 30, 2015)

The coarsening kinetics for the beading instability for liquid contained in a groove with convex curved sides (for example between a pair of parallel touching cylinders) is considered as an open channel flow problem. In contrast to a V-shaped wedge or U-shaped microchannel, it is argued that droplet coarsening takes place by viscous hydrodynamic transport through a stable column of liquid that coexists with the droplets in the groove at a slightly positive Laplace pressure. With some simplifying assumptions, this leads to a $t^{1/7}$ growth law for the characteristic droplet size as a function of time, and a $t^{-3/7}$ law for the decrease in the droplet line density. Some remarks are also made on the spreading kinetics of an isolated drop deposited in such a groove.

PACS numbers: 47.55.nb, 47.20.Dr

I. INTRODUCTION

Open channel flow problems have attracted much interest not only because of possible applications in microfluidics [1–9], but also because of their relevance to liquids spreading on topographically patterned surfaces such as human skin [10–12]. The paradigmatic case of spreading in a V-shaped wedge has been analysed both when liquid is supplied by a reservoir [10, 13], and in the starved (no reservoir) situation [14]. Various aspects of these predictions have been confirmed experimentally [2–4, 8]. Flows in U-shaped channels (*i. e.* with concave sides) have also been considered since such channels are easily micro-machined and are thus relevant for microfluidics applications [7, 11]. In the present study, I revisit the problem, in the context of a groove with *convex* sides, such as that formed between a pair of parallel touching cylinders (Fig. 1). In addition to possible microfluidics applications, interest in this problem is motivated by consideration of oily soil spreading along the fibres in textile yarns in woven fabrics [15]. It also has other potential technological relevance, for example to molten solder wicking in stranded copper wires and braids.

This problem throws up some interesting aspects not found in the previous cases. A groove with convex curved sides supports a stable uniform liquid column at low loads, but at higher loading a uniform liquid column may display a *beading instability* in which it breaks up into a string of droplets, similar to Rayleigh’s observation of the breakup of a thread of treacle on a paper surface [16]. Although the statics are by now quite well understood [5, 6, 9, 15, 17, 18], I shall argue here that the loading duality uniquely differentiates the present case from V-shaped wedges and U-shaped microchannels, since the droplets (beads) can coarsen by mass transport through connecting liquid columns.

Additionally, the loading duality implies an isolated droplet deposited into such a groove may show several

kinetic spreading stages as it empties into the unfilled regions. This aspect will be discussed at the end.

II. WICKING EQUATION

To start with, consider the general problem of open channel flow in a channel of arbitrary cross section, and let $A(x, t)$ be the cross section occupied by liquid. A local mass conservation law holds [13, 14, 19],

$$\frac{\partial A}{\partial t} + \frac{\partial(A\bar{v})}{\partial x} = 0. \quad (1)$$

Herein, the mean flow rate \bar{v} satisfies a Hagen-Poiseuille (HP) law, $\bar{v} = -(k/\eta)\partial p/\partial x$, in which k is the permeability (a quantity with units of length squared, *cf.* Darcy’s law), η is viscosity, and $p = p(A)$ is the (loading-dependent) Laplace pressure. Combining the HP law with Eq. (1) gives what can perhaps be called the *wicking equation*,

$$\frac{\partial A}{\partial t} = \frac{\partial}{\partial x} \left(\frac{Ak}{\eta} \frac{dp}{dA} \frac{\partial A}{\partial x} \right). \quad (2)$$

This is the basis for much of the subsequent development, and also codifies the statics *via* stability analysis. It generally has the character of a non-linear diffusion equation. I have assumed that the occupied cross section A is weakly varying with x , so the contribution to the Laplace pressure from the interface curvature in the longitudinal

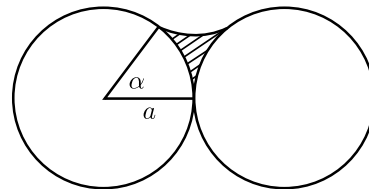


FIG. 1. Liquid in a groove between parallel touching cylinders.

* Email: patrick.warren@unilever.com

direction can be neglected. Note that the permeability also depends on the loading, so that $k = k(A)$.

Insight can be gained by linearising about the uniformly loaded static solution, *viz.* $A = A_0$ and $\bar{v} = 0$. Let us write $A/A_0 = 1 + \epsilon(x, t)$. Then $\partial\epsilon/\partial t = D_{\text{eff}} \partial^2\epsilon/\partial x^2$ where $D_{\text{eff}} = (Ak/\eta) dp/dA$ is an effective diffusion coefficient, evaluated at $A = A_0$. If this is positive, then perturbations will die away and the liquid will be self-levelling. If it is negative, then perturbations will grow indicative of the aforementioned beading instability. It is clear that the behavior depends, not on the sign of Laplace pressure p , but rather on the sign of dp/dA . Physically, if $dp/dA > 0$, an overfilled region will have a higher Laplace pressure than an underfilled region, and the liquid will flow to even things out. On the other hand, if $dp/dA < 0$, liquid will flow from underfilled regions into overfilled regions, magnifying the initial imbalance. The interesting and unusual property of a groove with convex curved sides is that both situations occur, depending on the loading.

III. STATICS

A specific example of the loading duality is provided by the groove between a pair of parallel touching cylinders, shown in Figs. 1 and 2. Since I neglect the interface curvature in the longitudinal direction, the transverse profile of the free surface is characterised by an arc of a circle with radius R . Taking $R > 0$ to indicate the surface is convex outwards, one has $p = \gamma/R$ where γ is surface tension. In this problem it is convenient [9] to parametrise the loading by the wrapping angle α , shown in Fig. 1. Note that the area is a monotonically increasing function of α , so $dA/d\alpha > 0$.

Elementary trigonometric arguments, first presented to my knowledge by Princen [15], show that

$$\frac{a}{R} = -\frac{\cos(\theta + \alpha)}{1 - \cos\alpha} \quad (3)$$

where θ is the liquid-solid contact angle. This result holds for both convex and concave interfaces, and the sign has been inserted in accord with the above convention that R is positive if the interface is convex.

From this we find (after a little rearrangement)

$$\frac{dR}{d\alpha} = -\frac{R^2 \cos(\frac{1}{2}\alpha + \theta)}{2a \sin^3(\frac{1}{2}\alpha)}. \quad (4)$$

Since $p \propto a/R$, Eqs. (3) and (4) show that p increases through zero at $\alpha + \theta = \frac{1}{2}\pi$ to reach a weak maximum at $\frac{1}{2}\alpha + \theta = \frac{1}{2}\pi$ (*i. e.* $\alpha = \pi - 2\theta$). A specific example is shown in Fig. 2a, for a contact angle $\theta = 30^\circ$. The zero crossing is at $\alpha = 60^\circ$ and the Laplace pressure maximum is at $\alpha = 120^\circ$. Fig. 2b shows a selection of the corresponding filling states. The stability requirement that $dp/dA \propto dp/d\alpha > 0$ indicates that filling states with $\alpha > 120^\circ$ are unstable with respect to the above-mentioned beading instability [20].

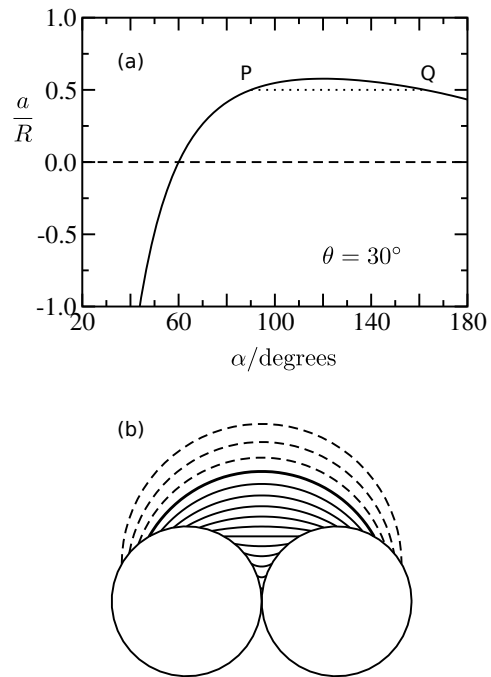


FIG. 2. (a) The dimensionless Laplace pressure as a function of the filling angle, with liquid-solid contact angle $\theta = 30^\circ$. (b) Filling stages in this problem: the thick solid line is the maximum Laplace pressure at $\alpha = 120^\circ$; uniform loading above this (dashed lines) is predicted to be unstable.

IV. KINETICS

A. Beading instability

As we have seen for the case of parallel touching cylinders, the Laplace pressure in a groove with convex sides may show a maximum as a function of the loading. Beyond the maximum, $dp/dA < 0$, and therefore a beading instability arises in which the uniformly loaded state is unstable towards the growth of perturbations. But first, what could be the final state in such a situation? In principle one can have two different states of loading at same Laplace pressure, which can therefore be in coexistence, for example points P and Q in in Fig. 2b. However the higher loaded state is always in the unstable region. The logical conclusion is that the excess liquid is expelled into a large droplet that sits somewhere on the two cylinders, coexisting with a stable column of liquid in the groove. In the case of parallel touching cylinders, the wrapping angle for this stable liquid column would have to satisfy $\frac{1}{2}\pi - \theta < \alpha < \pi - 2\theta$. The first inequality arises because the liquid column coexists with a large drop at a (weak) positive Laplace pressure [21]. The second inequality is the column stability condition.

I turn now to the coarsening kinetics. A uniformly overloaded state will certainly break up into a string of droplets, but in a groove with convex curved sides these

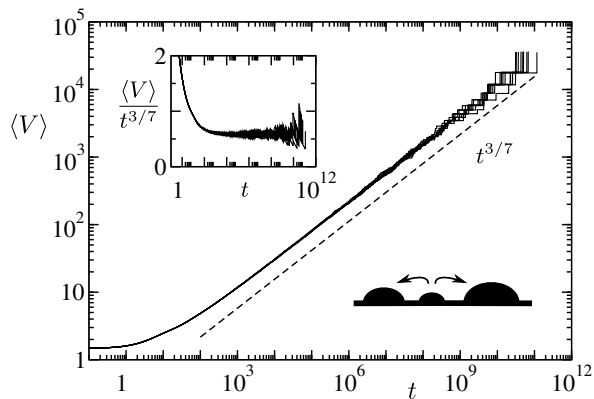


FIG. 3. Mean droplet volume as a function of time. Droplets coarsen by viscous hydrodynamic transport along the connecting liquid columns (diagrammatic inset), according to the rules prescribed in the Appendix. Results from 10 independent simulation runs are shown. Each simulation was initialised with 5×10^4 equispaced droplets, with random sizes taken from a uniform distribution $V_0 < V < 2V_0$. Droplets are removed when $V < 0.9V_0$, and their liberated contents are added to the liquid column ($\beta = 1$ in the model). The time step parameter was $\epsilon = 0.02$.

droplets are always connected by liquid columns with a finite filling depth according to the above argument. Therefore the larger droplets can eat the smaller ones, by transporting liquid along the connecting liquid columns. This stands in contrast to the V-shaped wedge for example, where spatially separated droplets are disconnected [4, 22, 23] and the droplet population has to coarsen by some other mechanism, such as a prewetting film [24–26], or transport through the vapor phase in the case of a volatile liquid.

With a simplifying assumption about how the Laplace pressure depends on the droplet size, aspects of the Lifshitz-Slyozov-Wagner (LSW) theory of droplet coarsening [27] can be adapted to the present case. The simplifying assumption is that the Laplace pressure scales inversely with droplet size as $p \propto V^{-1/3}$, where $V \equiv R^3$ is the droplet volume. This is likely to be true only asymptotically [28, 29]. Nonetheless, let us suppose that this is true, and the situation has evolved so that there is a string of droplets sitting in the groove. The following mean-field scaling *ansatz* predicts how the characteristic droplet size R , and characteristic spacing between droplets L , evolve with time.

First, the mass flux between adjacent droplets will be

$$J \sim \frac{a^4}{\eta} \frac{\Delta P}{L}. \quad (5)$$

This just expresses the HP law in scaling form. Shown here is the prefactor for the case of parallel touching cylinders, where the fourth power of the cylinder radius a arises from the product of the Darcy permeability $k \sim a^2$ and the cross sectional area of the connecting liquid column $A \sim a^2$. The analysis does not depend on this

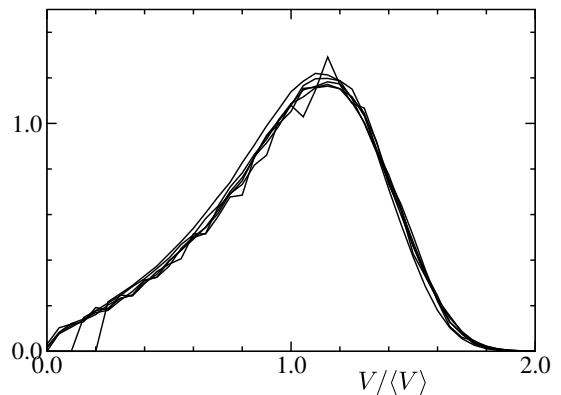


FIG. 4. Scale invariance of droplet size distribution. Histograms are computed when there are 10 000, 5000, 1000, 500, 300 and 100 droplets remaining out of an initial 5×10^4 , combining data from 100 independent simulation runs. Simulation parameters as for Fig. 3.

particular geometry though.

The mass flux is incorporated into a *local* mass conservation law, *cf.* Eq. (1), which governs the growth of the mean droplet volume,

$$\frac{dV}{dt} \sim J. \quad (6)$$

At the same time there is a *global* mass conservation law which relates the mean droplet size to the mean spacing,

$$\frac{V}{L} \sim \omega \sim \text{const}, \quad (7)$$

where ω is the mass per unit length [30].

Combining Eqs. (5)–(7), together with $V \equiv R^3$ and $\Delta p \sim \gamma/R$, shows that

$$R^2 \frac{dR}{dt} \sim \frac{\gamma a^4 \omega}{\eta R^4}. \quad (8)$$

This integrates to

$$R \sim \left(\frac{\gamma a^3 \omega t}{\eta} \right)^{1/7}. \quad (9)$$

Thus the prediction is that the mean droplet size should grow as $t^{1/7}$ and the droplet line density (*i. e.* $1/L \sim R^{-3}$) should diminish as $t^{-3/7}$.

The mean-field assumption is questionable given the one-dimensional nature of the coarsening problem. To investigate specifically just this aspect, I undertook numerical simulations using the model described in the Appendix. This confirms that the mean-field scaling *ansatz* does indeed predict how the mean droplet size grows with time (Fig. 3), and also demonstrates LSW-like scale invariance for the droplet size distribution (Fig. 4).

The origin of the mean-field behaviour is apparent if one examines the equal-time droplet size correlation function, $C(|i - j|)$, shown in Fig. 5. As can be seen the

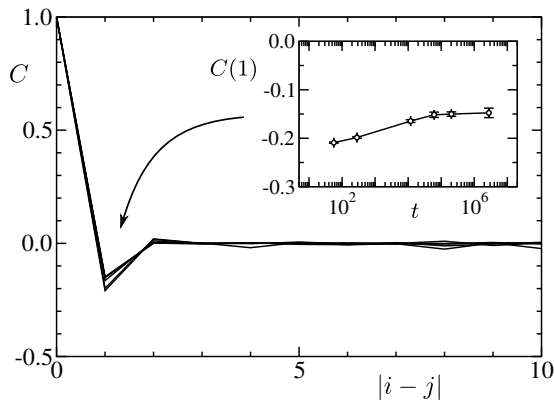


FIG. 5. Equal-time size correlation function, $C(|i-j|)$, computed for the same set of simulations used for Fig. 4. The inset shows the time dependence of the depth of the nearest-neighbour minimum. Error bars are from block averaging (10 blocks \times 10 runs).

only significant correlation appears to be between nearest neighbours, at $|i-j| = 1$. This indicates that droplets which are larger than average tend to be adjacent to droplets which are smaller than average, but apart from this no significant long-range correlations develop.

To see the origin of this nearest-neighbour correlation hole, consider an artificial situation in which one large droplet sits in a uniform string of equisized smaller droplets. Away from the large droplet, the ambient Laplace pressure is uniform and no coarsening takes place. However the large droplet has a sub-ambient Laplace pressure and so starts to draw in material from its immediate neighbours. This causes the immediate neighbours to shrink, and increases their Laplace pressure relative to the ambient background. The next-nearest neighbours then see that these droplets have started to shrink, and so they in turn start to grow. The process continues, and it is easy to see that it will generate a staggered array of droplet sizes, with a concomitant nearest-neighbour negative size correlation.

The nearest-neighbour correlation hole diminishes somewhat as time progresses, but eventually appears to settle down to a value $C(1) \approx -0.15$ (Fig. 5 inset). One should point out that the coarsening dynamics in the model is quite subtle, for instance, the largest droplet at time t may not necessarily be the largest droplet at some later time $t' > t$. This is because the growth rate of a droplet depends not only on its size but also on the sizes of its neighbours, and how far away they are.

B. Droplet spreading

The remaining point of kinetic interest concerns the fate of a droplet of liquid deposited onto an initially empty groove. The droplet will start to empty into the groove, presumably driving a Bell-Cameron-Lucas-

Washburn (BLCS) type flow from what is in effect a shrinking droplet reservoir [10, 13, 19]. This should persist all the way until the loading falls below the Laplace pressure maximum. Past this point, by analogy to the V-shaped wedge [14], one expects the spreading rate to slow down since the reservoir has been exhausted.

For the case of parallel touching cylinders, a second power law appears at a very late stage where everywhere $\alpha \ll 1$. In this limit, the wetted portion of the groove has shrunk to a narrow fissure with a width of the order $R \sim \alpha^2 a$ (see Eq. (3) in the limit $\alpha \rightarrow 0$) and a depth of the order αa . One therefore expects $A \sim \alpha^3 a^2$, and presumably $k \sim \alpha^4 a^2$ since the permeability should largely be determined by the width. Similar to the coarsening kinetics problem, a scaling analogue of the HP law can be introduced. In the present case this is $dL/dt \sim (k/\eta) \times \Delta p/L$ where L is the length of the wetted portion of the groove and $\Delta p \sim \gamma/R$ is the Laplace pressure. Substituting the above scaling expressions gives $dL/dt \sim \gamma \alpha^2 a / (\eta L)$. An additional constraint comes from the analogue of the global mass conservation law in Eq. (7), namely that the total droplet volume $\Omega \sim \alpha^3 a^2 L$ should be conserved. Eliminating α between this volume constraint and the HP scaling law yields $dL/dt \sim \gamma \Omega^{2/3} / (\eta a^{1/3} L^{5/3})$. This integrates to the final rather esoteric result

$$L \sim (\gamma t / \eta)^{3/8} \Omega^{1/4} a^{-1/8}. \quad (10)$$

In other words, the initial $L \sim t^{1/2}$ spreading law (BLCS) should weaken when the droplet reservoir vanishes, and eventually enter an $L \sim t^{3/8}$ power law in the final starved state.

V. DISCUSSION

I have argued that the kinetic aspects of spreading and (de)wetting for a liquid contained in a groove with convex curved sides presents some unique aspects when compared, for example, to a V-shaped wedge or a U-shaped microchannel. The novel aspects arise from an underlying loading duality, wherein a liquid column is stable at low loading, but becomes unstable at higher loading.

For the case of uniform loading above the critical loading threshold, a beading instability should be observed in which the liquid column breaks up into a string of droplets, which subsequently coarsen by mass transport along connecting liquid columns. With a simplifying assumption about the dependence of the Laplace pressure on the droplet volume, a mean-field scaling *ansatz* indicates that the droplet size and line density scale with non-trivial power laws in time, and simulations show that this is not destroyed by the one-dimensional nature of the problem.

Of course, the simplifying assumption about the Laplace pressure scaling does not hold in reality, and in general I would expect the clean power law behaviour to be modified by finite-droplet-size effects, which may be

quite persistent. Some general predictions should be robust however, such as the relatively slow droplet growth *via* transport along connecting liquid columns, and the negative correlation between nearest neighbour droplet sizes shown in Fig. 5. These could perhaps be tested in an electrowetting experiment [3, 4]. I should caution that the predicted slow coarsening kinetics may be overtaken by other, ultimately faster, mechanisms. For example transport through the vapour phase for a volatile liquid may ultimately lead to a $R \sim t^{1/3}$ coarsening law, as in LSW theory [27].

Another prediction arising from the loading duality is that a droplet deposited in the groove should show a staged spreading kinetics, starting with the classic Bell-Cameron-Lucas-Washburn law as the droplet initially acts like a reservoir, slowing when the loading falls everywhere below the critical value, and possibly ending with a new power law in the final starved state. Again, this may perhaps be probed experimentally.

Appendix A: Simulation of coarsening kinetics

I introduce a simplified model of the coarsening kinetics to test specifically the mean-field *ansatz* presented in the main text. In the model, I consider a one-dimensional string of $i = 1 \dots N$ droplets, connected by liquid columns as indicated in the lower inset in Fig. 3. Big droplets grow, and small droplets shrink, under the influence of viscous hydrodynamic transport through the liquid columns. This is driven by differences in the Laplace pressure between neighbouring droplets. To establish a system of kinetic equations for the droplet sizes, I suppose that the Laplace pressure in the i -th droplet is proportional to $V_i^{-1/3}$, where V_i is the droplet volume (this is the simplifying assumption mentioned in the main text). According to the HP law, the Laplace pressure difference drives a mass flux through the connecting liquid column as, *cf.* Eq. (5),

$$J_i = \frac{V_i^{-1/3} - V_{i+1}^{-1/3}}{L_i}. \quad (\text{A1})$$

In this L_i is the distance between the i -th and $(i+1)$ -th droplets, and all other material properties in the problem have been subsumed into the definitions of length, volume and time. Note that $V_{i+1} > V_i$ implies $J_i > 0$, so that liquid flows from smaller droplets to larger droplets. Given the fluxes, mass conservation dictates that, *cf.* Eq. (6),

$$\frac{dV_i}{dt} = J_{i-1} - J_i. \quad (\text{A2})$$

Eqs. (A1) and (A2) are the required set of non-linear kinetic equations. Since they predict that droplets shrink, as well as grow, we need a rule which governs how shrinking droplets can disappear. At this point it is convenient to introduce a fiducial volume $V_0 \sim R_0^3$, where the fiducial length R_0 is set by the height of the connecting liquid column (in the simulations, $V_0 = R_0 = 1$). A simple rule for shrinking droplets is that they vanish when $V_i < \alpha V_0$. If this happens, the droplet is removed and the distance between the remaining droplets is set equal to $L_{i-1} + L_i + \beta V_i^{1/3}$, where the third term is an *ad hoc* correction for the length contributed by the vanished droplet (taking β as a free parameter).

As an initial condition I set $V_i = r_i V_0$ where r_i is a random number chosen from a uniform distribution, $1 \leq r_i < r_m$. The droplets are initially equispaced, with $L_i = R_0$. Periodic boundary conditions are imposed.

The droplet volumes are evolved according to Eqs. (A1) and (A2), alongside the above rule for removing droplets which become too small. Eqs. (A1) and (A2) are integrated using a simple, adaptive, Euler-type forward finite difference scheme, with a time step Δt chosen such $dV_i/dt \times \Delta t/V_i \leq \epsilon$, in other words so that the fractional change in any droplet size does not exceed ϵ in any time step. For the reported simulations I used $\alpha = 0.9$ and $\beta = 1$ for the vanishing rule, $r_m = 2$ for the maximum initial drop size relative to V_0 , and $\epsilon = 0.02$ for the choice of time step. I have checked the results are insensitive to these choices.

As time evolves, the larger droplets grow at the expense of the smaller droplets, and the smallest droplets shrink and vanish. Eventually the simulation stops when there is one large final droplet ($N = 1$). I monitor the mean droplet volume $\langle V \rangle = (1/N) \sum_{i=1}^N V_i$ as a function of time (note that N changes as droplets disappear), and at selected time points record the drop size distribution. Typical results, aggregated from multiple simulation runs from independent starting points, are summarised in Figs. 3 and 4.

I also calculate periodically the equal-time correlation function

$$C(|i-j|) = \frac{\langle \Delta V_i \Delta V_j \rangle}{\langle \Delta V^2 \rangle}, \quad (\text{A3})$$

where $\Delta V_i = V_i - \langle V \rangle$ is the deviation from the mean droplet volume, at time t . This function is shown in Fig. 5, evaluated at various points in the simulation.

[1] T. M. Squires and S. R. Quake, Rev. Mod. Phys. **77**, 977 (2005).
 [2] J.-C. Baret, M. M. J. Decré, S. Herminghaus, and R. See-

mann, Langmuir **23**, 5200 (2007).
 [3] K. Khare, *et al.* Langmuir **23**, 12997 (2007).
 [4] K. Khare, *et al.* Eur. Phys. J. Special Topics **166**, 151

- (2009).
- [5] X.-F. Wu, A. Bedarkar, and K. A. Vaynberg, *J. Colloid Interface Sci.* **341**, 326 (2010).
- [6] A. Bedarkar, X.-F. Wu, and A. Vaynberg, *Appl. Surf. Sci.* **256**, 7260 (2010).
- [7] D. Yang, *et al.* *J. Phys. Chem. C* **115**, 18761 (2011).
- [8] J. Barman, *et al.* *Langmuir* **31**, 1231 (2015).
- [9] A. Sauret, *et al.* *Soft Matter* **11**, 4034 (2015).
- [10] A. D. Dussaud, P. M. Adler, and A. Lips, *Langmuir* **19**, 7341 (2003).
- [11] Y. Chena, *et al.* *Micro. Engn.* **86**, 1317 (2009).
- [12] R. Seemann, M. Brinkmann, S. Herminghaus, K. Khare, B. M. Law, S. McBride, K. Kostourou, E. Gurevich, S. Bommer, C. Herrmann, and D. Michler, *J. Phys.: Condens. Mat.* **23**, 184108 (2011).
- [13] L. A. Romero and F. G. Yost, *J. Fluid Mech.* **322**, 109 (1996).
- [14] P. B. Warren, *Phys. Rev. E* **69**, 041601 (2004).
- [15] H. M. Princen, *J. Colloid Interface Sci.* **34**, 171 (1970).
- [16] Lord Rayleigh, *Phil. Mag.* **34**, 145 (1892).
- [17] A. E. Sáez and R. G. Carbonell, *J. Fluid Mech.* **176**, 357 (1987).
- [18] C. Duprat, A. D. Bick, P. B. Warren, and H. A. Stone, *Langmuir* **29**, 7857 (2013).
- [19] M. Reyssat, L. Courbin, E. Reyssat, and H. A. Stone, *J. Fluid Mech.* **615**, 335 (2008).
- [20] An interesting corollary is that the maximum stable filled state may protrude above the cylinders (*cf.* the heavy filled line in Fig. 2b). For parallel touching cylinders one can show that this occurs if the contact angle is *smaller* than 60° . The behavior stands in marked contrast to the influence of contact angle on the height of a droplet sitting as a spherical cap on a flat surface. This consideration potentially influences the wicking of liquids in woven fibrous networks, bearing in mind the applications mentioned in the introduction.
- [21] A consequence of this is that as more liquid is added, the amount contained in the groove should go *down*, since adding liquid increases the size of the large droplet and reduces its Laplace pressure (towards zero), thereby in parallel diminishing the loading in the liquid column contained in the groove.
- [22] P. Concus and R. Finn, *Proc. Natl. Acad. Sci. (USA)* **63**, 292 (1969).
- [23] K. Rejmer, S. Dietrich, and M. Napiórkowski, *Phys. Rev. E* **60**, 4027 (1999).
- [24] A. O. Parry, C. Rascón, and A. J. Wood, *Phys. Rev. Lett.* **85**, 345 (2000).
- [25] J. M. Romero-Enrique and A. O. Parry, *New J. Phys.* **9**, 167 (2007).
- [26] A. Malijevský and A. O. Parry, *Phys. Rev. Lett.* **110**, 166101 (2013).
- [27] A. J. Bray, *Adv. Phys.* **43**, 357 (1994).
- [28] B. J. Carroll, *J. Colloid Interface Sci.* **57**, 488 (1976).
- [29] P. G. de Gennes, F. Brochard-Wyart, and D. Quéré, *Capillarity and Wetting Phenomena* (Springer, New York, 2004).
- [30] It seems likely that $\omega \equiv R^3/L \sim a^2$ since this is the only length scale. This would correspond to an initial droplet volume of order a^3 and droplet spacing of order a .